공학석사학위논문

Paintable decellularized-ECM hydrogel for cardiac tissue augmentation in myocardial infarction model

심근 경색 모델에서의 심장 조직 증대를 위한 페인터블 탈세포 세포외기질 하이드로겔

2023 년 2 월

서울대학교 대학원
화학생물공학부

이 재 우

공학석사학위논문

Paintable decellularized-ECM hydrogel for cardiac tissue augmentation in myocardial infarction model

심근 경색 모델에서의 심장 조직 증대를 위한 페인터블 탈세포 세포외기질 하이드로겔

2023 년 2 월

서울대학교 대학원
화학생물공학부

이 재 우

Paintable decellularized-ECM hydrogel for cardiac tissue augmentation in myocardial infarction model

심근 경색 모델에서의 심장 조직 증대를 위한
페인터블 탈세포 세포외기질 하이드로겔

지도교수 황 석 연

이 논문을 공학석사 학위논문으로 제출함

2023 년 2 월

서울대학교 대학원
화학생물공학부
이 재 우

이재우의 석사학위논문을 인준함

2023 년 2 월

위 원 장 김 병 기 (인)

부위원장 황 석 연 (인)

위 원 김 병 수 (인)

Abstract

Paintable decellularized-ECM hydrogel for cardiac tissue augmentation in myocardial infarction model

Jaewoo Lee

School of Chemical and Biological Engineering

The Graduate School of Engineering

Seoul National University

Myocardial infarction (MI) is a cardiovascular disease that causes thinning of the ventricular wall, loss of cardiac function, and heart failure due to heart muscle necrosis occurred by decreasing blood flow to the coronary artery of the heart. Currently, studies using injectable biomaterials or patches that require additional treatment, such as sutures, limit MI recovery due to secondary damage. Here, paintable hydrogel containing heart-decellularized extracellular matrix (hdECM) can be conveniently painted onto the round beating heart without secondary damage to the tissue. hdECM provides a heart-like environment to induce differentiation of cardiomyoblasts and induces blood vessels in necrotic tissues through cell infiltration of epithelial cells, thereby obtaining the effect of tissue regeneration This tyramine conjugated hyaluronic acid (HA_Tyr) based paintable hydrogel exhibits robust adhesion strength on wet surfaces by tyrosinase-catalyzed oxidative reaction, adequate swelling ratio, and sufficient mechanical strength to assist heart beating. In

addition, in vivo, the hdECM-containing paintable hydrogel is maintained for 28 days with high stability and adhesiveness, reduces fibrosis and thinning of the ventricular wall in the MI region, and induces angiogenesis by hdECM, leading to effective myocardial infarction repair. Overall, the hdECM-containing paintable hydrogel, which is simply applied and has a cardiac tissue-specific environment, treats MI with adequate mechanical strength and angiogenic ability.

Keyword : Decellularization, Paintable, Hydrogel, Myocardial infarction

Student Number **: 2021-24083**

Contents

Abstract i

Contents iii

List of Figures and tables 1

Chapter 1. The scientific background 3

1.1. Myocardial infarction (MI) 3

1.2. Decellularization 4

1.2.1. Extracellular matrix (ECM) 4

1.2.2. Decellularized Extracellular Matrix (dECM) 5

1.3. Bio-functional hydrogels 6

1.4. *Streptomyces avermitilis*-derived tyrosinase (SaTy) 8

1.5 Research aims 9

Chapter 2. Experiment Section 11

2.1. Materials 11

2.2. Methods 11

2.2.1. Decellularization of porcine heart 11

2.2.2. Biochemical characterization of hdECM 12

2.2.3. Synthesis of paintable hydrogel 12

2.2.4. Synthesis and purification of SA_ty 13

2.2.5. Measurement of adhesiveness 14

2.2.6. Swelling behavior of HA_tyr hydrogel 15

2.2.7. Compression properties of paintable hydrogel 15

2.2.8. Rheological behavior of HA_Tyr hydrogel 15

2.2.9. Degradation behavior of HA_Tyr hydrogel 16

2.2.10. Live/Dead Assay 16

2.2.11. MI Modeling in Rats and Hydrogel Painting 17

2.2.12. Masson's Trichrome (MT) Staining 18

2.2.13. Immunofluorescence (IF) Staining 18

Chapter 3. Results and Discussions 20

3.1. Decellularization 20

3.1.1. Optimize decellularization solution concentration 20

3.1.2. Quantification of ECM components and DNA 24

3.2. Paintable hydrogel 25

3.2.1. Synthesis of paintable hydrogel 25

3.2.2. Specific activity of SA_Ty 27

3.2.2. Optimize concentration of HA_Tyr hydrogel 28

3.2.3. Swelling property of the paintable hydrogel 31

3.2.4. Mechanical strength of the swollen paintable hydrogel 33

3.2.5. Adhesion loss of paintable hydrogel 34

3.2.6. Radical scavenging activity of paintable hydrogel 38

3.3. In vitro analysis 38

3.3.1. Cell viability 38

3.3.2. Cell differentiation 40

3.4. In vivo analysis 42

3.4.1. Degradation behaviors of paintable hydrogel 42

3.4.2. Paintable hydrogel treatment on the MI-induced heart 44

3.4.3. Histological analysis 45

3.4.4. Cell infiltration and angiogenesis 46

3.4. In vivo analysis 47

Chapter 4. Conclusion 49

References 50

Abstract in Korean 52

List of Figures and tables

Figure 1. Overall scheme of hdECM-based paintable hydrogel

Figure 2. Optical images of native and decellularized mouse hearts

Figure 3. Optical images of native and decellularized porcine hearts

Figure 4. Weight remaining in the process of decellularization in different SDS concentrations

Figure 5. H&E staining of native and decellularized porcine hearts

Figure 6. F-actin staining of native and decellularized porcine hearts

Figure 7. Quantification of ECM components (GAG and collagen) and DNA in different SDS concentrations.

Figure 8. 300MHz HNMR of HA and HA_Tyr

Figure 9. Mechanism of HA_tyr polarization

Figure 10. FT-IR of HA_Tyr and crosslinked HA_tyr

Figure 11. Specific activities of SA_Ty to monophenolic compound, L-tyrosine (Left) and tyramine (Right)

Figure 12. Paintability in the diverse concentration of HA_tyr

Figure 13. Painting on the paper and PDMS mold

Figure 14. Adhesiveness of HA_Tyr with diverse concentration

Figure 15. Viscosity of each step of HA_tyr gelation

Figure 16. Swelling behaviors of paintable hydrogel pellets

Figure 17. Swelling ratio of paintable hydrogel pellets

Figure 18. Compressive strength of the paintable hydrogel

Figure 19. Amplitude sweep in rheological analysis

Figure 20. Frequency sweep in rheological analysis

Figure 21. Scheme of losing surface adhesion of paintable hydrogel

Figure 22. Tissue adhesion mechanism of the catechol group

Figure 23. Quantification of radicals with or without washing

Figure 24. Adhesion test of paintable hydrogel on the weighing dish

Figure 25. Adhesive strength of the paintable hydrogel

Figure 26. Radical scavenging of paintable hydrogel compounds

Figure 27. Live dead assay with paintable hydrogel extract

Figure 28. Cell viability ratio with paintable hydrogel extract

Figure 29. Differentiation of cardiomyoblast with paintable hydrogel extract

Figure 30. Cell orientations of cardiomyoblast

Figure 31. Cell circularity of cardiomyoblast

Figure 32. Weight remaining in the PBS and enzymatic condition

Figure 33. Weight remaining in the mice subcutaneous

Figure 34. MI-inducing and paintable hydrogel treatment

Figure 35. Induced MI and hydrogel-painted region

Figure 36. MT staining after 4 weeks (Whole organ)

Figure 37. MT staining after 4 weeks (MI-induced region)

Figure 38. Cardiomyocyte infiltration and angiogenesis

Figure 39. Paintable hydrogel adhesiveness on the porcine heart

Table 1. Kinetic parameters of SA_Ty for substrate L-tyrosine and tyramine.

Chapter 1. The scientific background

1.1. Myocardial infarction (MI)

The heart which has an organized fibrillar structure acts as a muscular pump that continuously provides blood throughout the body and its' mechanical strain exceeds 20% between systole and diastole within the left ventricle. [1] Although the heart has an important role in our body, the heart is the least regenerative organ than any other organ. [2] Myocardial infarction (MI), one of the most acute diseases in cardiovascular tissue, is a typical ischemia heart due to the blockage of a coronary artery that reduces the blood supply to the heart. Then, MI causes oxygen deprivation of the affected tissue, leading to tissue necrosis and cardiomyocyte loss due to a necrotic and apoptotic environment. [3] Massive cardiomyocyte loss after MI leads to abnormal ventricular remodeling, including ventricular wall thinning, local area stiffening, and scar tissue formation. In addition, increased matrix metalloproteinases from inflammatory infiltrate degrade extracellular matrix (ECM), further exacerbating cardiac decline and subsequently causing deposition of fibrillar cross-linked collagen. [4] Also, Scarring and fibrosis by MI lead to maladaptive remodeling and hypertrophic expansion of the ventricles leading to inefficient contractile and reduced cardiac output. The overall situation can lead to loss of normal contractility and function, leading to death and disability. [5]

1.2. Decellularization

1.2.1. Extracellular matrix (ECM)

Multicellular microstructures found in tissues include collagen fibers, microfibrils, sheets, and cell spheroids. These structures collaborate with other ECM proteins to form various connective tissues. [6] Furthermore, the ECM has biochemical and mechanical properties that influence cell behaviors, mature, and response to injury. More specifically, the ECM interacts with growth factors and signaling molecules via its biochemical properties to control cellular functions such as cell adhesion, proliferation, differentiation, migration, survival, and survival. The differentiation and migration leading cells to divide and gather into tissues with distinct functions are accompanied by the dynamic remodeling of the ECM into tissue-specific 3D architectures and compositions. [7] Through its mechanical properties, ECM acts as a scaffold that maintains the structural integrity of multicellular organisms, promotes the interaction between individual cells and between different cell types and its elasticity/stiffness affects cellular differentiation. [8] The important point is that the ECM of each tissue has tissue-specific composition and topology due to dynamic interactions between the resident cells and the microenvironment. [9] By using tissue-specific ECM materials in tissue engineering facilitates constructive remodeling and recreates more complex biologically and biochemically relevant microenvironment.

1.2.2. Decellularized Extracellular Matrix (dECM)

The diversity of tissue-specific ECM provides unique structural characteristics and biophysical and biochemical components. [6] Moreover, several studies have demonstrated the efficacy of tissue-specific ECM. [10] [11] However, simple implantation of ECM causes acute rejection because the foreign molecule is recognized by the immune system. In this aspect, decellularization is the process of removing cellular antigens from tissues that initiate an immune response with intact ECM containing a mixture of structural and functional molecules. In the past, dECMs had normally been considered for autograft, allograft and xenograft by whole organ decellularization with perfusion. Since autograft dECM has tissue limitations, most dECMs are from allogeneic or xenogeneic donor tissues. However, still there are several problems, such as the number of available donor organs, donor site morbidity, architecture and mass composition differences, which exist in allogeneic/xenogeneic dECM. Recently, dECM, instead of transplantation, is used for tissue-specific biomaterial.

According to its purpose, the decellularization process has to remove cellular components representing an optimal 98% reduction with maintaining tissue-specific biochemical composition for the remaining ultrastructure architecture and mechanical properties of the native ECM. [9] There are various decellularization methods to meet these conditions. First, the physical decellularization method modulates physical properties such as temperature and pressure to disruption of cell membranes and removes cell contents. Second, the chemical decellularization method uses detergents and chemicals to disrupt the attachment of cells and remove cellular components. Third, ionic, nonionic and zwitterionic surfactants are

amphiphile compounds that can interfere between hydrophobic molecules and hydrophilic molecules. Surfactants solubilize cell membranes and separate DNA from proteins and remove cellular components. Fourth, acids and bases catalyze the hydrolytic degradation of biomolecules and cellular components, such as cytoplasmic components and nucleic acids. However, acid can decompose the ECM microstructure, reduces collagen, and weakens tissue mechanical properties. Alkali can reduce GAG content and eliminate growth factors. Last, the enzymatic decellularization method has high specificity for decellularization by cleaving specific strands within cell or cell-matrix junctions. Despite these various decellularization methods, there is no methodological gold standard for decellularization as the decellularization process is highly dependent on the conditions of the tissue such as species, anatomical location and size. Therefore, optimization of decellularization methods is essential depending on tissue conditions.

1.3. Bio-functional hydrogels

Biological scaffolds, especially hydrogels, have high biocompatibility and bioactivity and cell differentiation ability depends on their mechanical properties. [12] For example, mesenchymal stem cells grown in soft hydrogels differentiate into neuronal-like lineages, whereas those grown in stiff hydrogels differentiate into osteoblastic lineages. [13] Also, hydrogels are widely used in biomedical regenerations due to their high-water content and biocompatibility. [14] However, there are still some of the hurdles in tissue repair ability, such as immunogenicity overcoming, in vivo microenvironment simulation and similar mechanical or

biochemical properties to native tissues. To overcome these limitations, current researches incorporate bioactive molecules, such as growth factors, cytokines and dECM with tissue-engineered hydrogels. Hydrogel application methods can be classified into several. First, injectable hydrogels, which have the lowest viscosity, are usually applied through the syringe injection. For this reason, the injectable hydrogel is minimally invasive and completely fills the defects but it is hard to use for the drug sustained release and has low mechanical strength. Second, patches are fabricated by utilizing manufacturing techniques, such as electrospinning and 3D bioprinting. Their 3D scaffolds have high-fidelity nanoscale topography and bioactivity, and can mimic both the appearance and internal structure of the native tissues. However, every application method has proper target tissue to apply. For example, in the case of bone tissue, hydrogel which has high mechanical strength should be employed and low-viscosity hydrogel is applied for the cavity defects. In this aspect, for the heart, the fabricated hydrogel has to have stable and strong adhesion properties because of the continued heart beating. Most adhesive hydrogels employ covalent bonds between the hydrogel and the tissue surface. Covalent bonding which uses in hydrogel adhesion is done by reactive groups, such as NHS ester [15], aldehyde [16], and catechol [17]. The catechol groups are oxidized into catechol quinones, which can react with other functional groups, such as thiols, amines, and other catechol groups. Oxidized catechol provides strong adhesion to wet surfaces [18] and produces quinone-polymerized products by crosslinking reaction. [19] Two methods for facilitating crosslinking reactions based on oxidation catechol groups are horseradish peroxidase (HRP) and chemical oxidation with sodium periodate ($NaIO_4$). [20] [21]. These methods have a limited range of viable applications due to the cytotoxicity and pH sensitivity of the chemical reagents. In a

previous study, recombinant tyrosinase from Streptomyces avermitilis (SA Ty) was used as a crosslinking agent with macromolecule selectivity and high reactivity. [14]

1.4. *Streptomyces avermitilis*-derived tyrosinase (SaTy)

Crosslinking is used to increase mechanical strength and ensure a stable 3D network structure. Cross-linking reactions based on oxidized phenol groups can be promoted by various strategies including chemical oxidation by $NaIO_4$ or enzymatic activation by HRP. However, these approaches are of limited practical application since only phenolic couplings can be used for cross-linking, as well as the cytotoxicity and pH dependence of chemical reagents. Tyrosinase, a key enzyme in melanin synthesis, is an amine adjacent to the enzyme that converts L-tyrosine to L-3,4-dihydroxyphenylalanine (L-DOPA). Phenolic groups combine with certain thiols or form melanin. [19] During subsequent oxidation, two separate catechols are converted to quinones that are spontaneously oxidized to quinone polymerization products. Tyrosinase is a type 3 copper oxygenase catalyzed by an ortho-diphenol on the phenolic moiety followed by an orthoquinone. [22] A unique enzymatic mechanism mediated by bound cupric ions allows the substrate to be directly oxidized by molecular oxygen. Tyrosinase oxidizes o-diphenols to reactive o-quinones in humid environments and combines with amines, thiols, imidazoles and other quinone groups. Moreover, SaTy-based hydrogel systems show great potential as tissue adhesives and materials for tissue regeneration. [23] [24]

1.5 Research aims

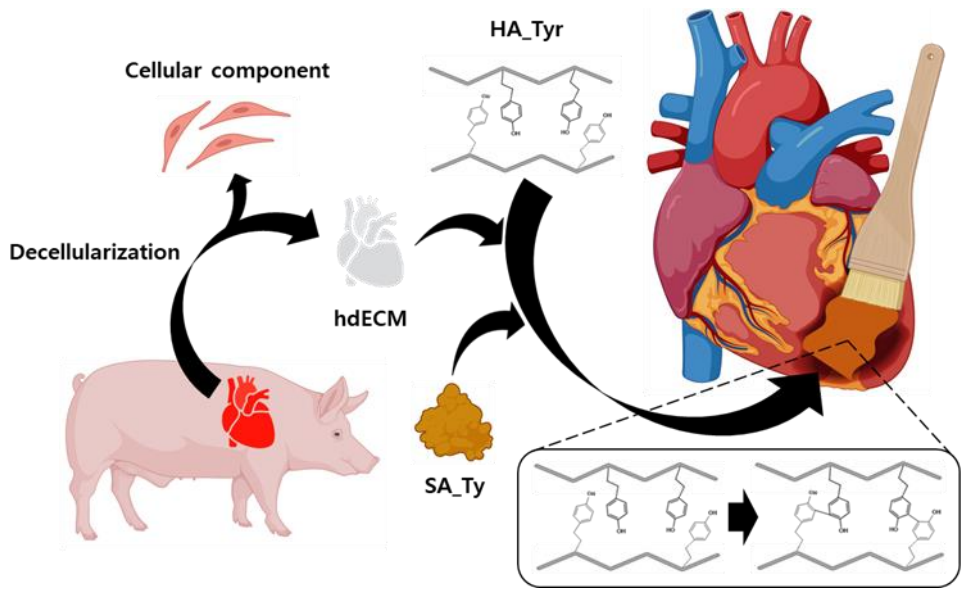

Figure 1. Overall scheme of hdECM-based paintable hydrogel

Recent studies in MI mainly apply two types of hydrogels: injectable hydrogels and patches. First, the injectable hydrogel was applied directly to the left ventricular (LV) wall or use chamber/transcatheter injection. However, injectable hydrogels have limitations. For example, injectable hydrogels typically use a needle, which causes new damage to the beating heart. Second, patches have been developed to treat myocardial infarction. However, patches were sutured to the myocardium or required a light-triggered response because of their low adhesiveness. Also, those inevitably cause new damage to the heart. In this aspect, adhesive hydrogels were chosen as an alternative to sutures because they readily attach to tissue through functional groups and chemical bonds on the tissue surface. By using adhesive hydrogel, the paintable adhesive hydrogel was recently utilized. [12] The paintable adhesive hydrogels

rapidly bonded to beating non-flat heart tissue in an uncomplicated manner without further processing, such as sutures. However, synthetic hydrogels fail to exhibit the complexity of native ECM and are inadequate to recapitulate microenvironments with cell interactions. [9] To develop the paintable hydrogel for MI, tissue-specific dECM was added to the hydrogel. Recent studies have validated tissue-specific dECM and demonstrated functional enhancement and tissue regeneration when using tissue-specific ECM scaffolds. [25] Moreover, ECM materials that act as physical scaffolds interact with individual cells, mimic tissue-specific biophysical and biochemical organization, and facilitate constructive remodeling at the implantation site. [26] And paintable hydrogel which contains cardiac dECM can promote revascularization of the defect region, regulate cardiomyocyte proliferation and differentiation, and induce cardiac tissue remodeling. [27] In this study, I utilized tyramine conjugated hyaluronic acid (HA_Tyr) based paintable hydrogel with cardiac tissue-specific heart-decellularized extracellular matrix (hdECM). I observed prevented thinning of the ventricular wall and induced angiogenesis by simply delivering the hdECM scaffold by painting. The application of tissue-specific ECM provides an important role in cell engraftment, survival, and adaptive function **(Figure 1).**

Chapter 2. Experiment Section

2.1. Materials

As synthetic biomaterials, Hyaluronic acid (Molecular weight = 1,000-1,200 kDa, NutriVita, USA) was used. Tyramine hydrochloride, pepsin and Triton X-100 were purchased from Sigma-Aldrich (Seoul, Korea). 4-(4,6-Dimethoxy-1,3,5-triazine-2-yl)-4-methylmorpholinium Chloride (DMTMM) was purchased from Tokyo Chemical Industry Co., Ltd (TCI, Tokyo, Japan), Porcine Heart was purchased from Biozoa (Seoul, Korea), Sodium dodecyl sulfate (SDS) was purchased from Bio-Rad (California, USA). The porcine heart was obtained from a slaughterhouse

2.2. Methods

2.2.1. Decellularization of porcine heart

The porcine heart was obtained from a slaughterhouse and the Sliced porcine heart in 3 mm thick. The sliced heart was washed with cold distilled water for a day to remove the blood. Proceed with decellularization to treat with 1% SDS for 48 hours and treated with 1% Triton X-100 for 6 hours. Triton X-100 effectively eliminates the residual SDS. The decellularized heart was sterilized with 0.1% peracetic acid in 4% ethanol for 4 hours and washed with sterilized distilled water for 6 hours. The lyophilized decellularized heart was digested with pepsin (decellularized heart : pepsin = 10:1, weight ratio) in 0.5M acetic acid. Pepsin digestion cleaves the

telopeptide region of COL, allowing the dissolution of dECM in dilute acid. [9] Neutralize digested solution into to physiological pH (pH 7.0) and lyophilized for 3 days. Pulverized lyophilized hdECM with a blender to obtain hdECM powder and stored in a -80℃ deep freezer.

2.2.2. Biochemical characterization of hdECM

To verify the extent of decellularization, residual DNA and ECM components were measured through biochemical assay and hematoxylin & Eosin (H&E) staining. For the biochemical assay, the native porcine heart was digested in the same method as a decellularized heart. Residual DNA was quantitatively evaluated by using Quant-iT™ PicoGreen™ dsDNA Assay Kit (Thermofisher) following the manufacturer's process. The quantification of collagen was measured by the hydroxyproline assay, and the quantification of GAG was measured by the 1,9-dimethyl methylene blue (DMMB) assay, as described in the previous studies. [24] Absorbance or fluorescence measurements were conducted by spectrophotometer (TECAN, Switzerland). For histological evaluation, both native and decellularized tissues were fixed in 4% paraformaldehyde for a day. After washing several times, tissues were dehydrated, embedded in paraffin, sectioned using a cryotome (Leica RM2125 RTS, Germany), stained with H&E, and observed using a microscope (Nikon, Japan).

2.2.3. Synthesis of paintable hydrogel

Carbodiimide chemistry is commonly used to prepare HA–catechol. It involves the formation of an amide bond between the carboxylic group of HA and the amine of

tyramine. The amide bonds between tyramine and the carboxyl group of HA were mediated by DMTMM. Briefly, 1g of HA sodium salt was dissolved into 100 ml of pH 5.5 MES buffer. When the temperature of the solution reaches 70℃, DMTMM is added in molar ratio HA : DMTMM = 1 : 2 and reacted for 30 minutes. The temperature of the solution was lowered to RT, and tyramine was added in molar ratio HA : tyramine = 1:4, followed by a reaction for 24 hours. After dialysis for 2 days, lyophilization was performed for 3 days to obtain the HA_Tyr. The degree of substitution (DS) of the tyramine was measured by 1HNMR (AVANCE Ⅲ HD 300MHz). FT-IR spectra were measured at wavelengths from 400 to 4000 cm-1 using an FT-IR spectrometer. (Bruker TENSOR27).

2.2.4. Synthesis and purification of SA_ty

Tyrosinase E-coli was inoculated with ampicillin in autoclaved LB medium and grown overnight in a shaking incubator at 37℃. The grown E-coli s transferred to autoclaved LB medium with ampicillin and grown in a shaking incubator at 37℃ for 3 hours. When the OD600 value of the bacteria solution is between 0.6 and 0.8, add 1M isopropyl β-D-1-thiogalactopyranoside (IPTG) and 1M CuSO4*5H2O, and synthesize tyrosinase in a shaking incubator at 18℃ for 20 hours. Cell pellets were collected by ultra-centrifugation and washed with 5ml of 50mM tris-HCl buffer at pH 8 twice. The cells were lysate by ultra-sonicator (VC505, USA) at 4℃ for 20min. After centrifugation at 4℃ for 30min. The expressed enzymes were purified by the general His-tag purification with Ni-NTA agarose bead. Tyrosinase was collected by a 10kDa filter tube and mixed with autoclaved 75% glycerol solution after 0.22μm syringe filtration. To evaluate the activity of SA_Ty, the concentration of purified

enzymes was calculated by the general Bradford assay. After adding pH 8.0 tris buffer, 10 nM CuSO4, tyrosinase, and 2 mM L-tyrosine, incubated at 37°C for 30 minutes and measured absorbance at 475 nm. The specific activity of SA_ty was calculated using the Beer-Lambert law and the initial rate of tyrosinase was determined by measuring the several concentrations of L-tyrosine and tyramine at 475 nm with UV-spectroscopy at 37°C.

2.2.5. Measurement of adhesiveness

First, HA_tyr was dissolved in DW at concentrations of 1%, 2%, and 4% (w/v), and hdECM was mixed at a concentration of 1% (w/w). Proceed with cross-linking by mixing SA_Ty. To measure tensile strength, adhered samples with adhesion areas of width 2.5 cm and length 2.5 cm were prepared and tested by the standard tensile test (ASTM F2258) with a mechanical testing machine (2.5 kN load-cell, Zwick/Roell Z2.5). All tests were conducted with a constant tensile speed of 50 mm min−1. Tensile strength was determined by dividing the maximum force by the adhesion area. To measure the tensile strength, an adhesion area of 2.5 cm in width and 2.5 cm in length was prepared and subjected to a standard tensile test (ASTM F2258). All tests were performed at the constant tensile speed of 50 mm min^{-1}. 3D printed holder were applied using glues to provide grips for tensile tests. In the case of washed samples, after cross-linking was completed, samples were washed three times with PBS and measured. Lap-shear test (ASTM F2255) and tensile test (ASTM F2258) were performed to measure the adhesiveness of hydrogel by using porcine skin and LV ventricular wall. [25] The porcine skin and ventricular wall were cut into similar sizes (fixed at 2.5 cm ×2.5 cm) and glued or fixed on both sides of UTM (Shimazu,

EZ-SX STD, Japan) modules. Before measurement, HA_Tyr hydrogel was painted on the single side of the porcine skin and ventricular wall. The samples were pulled to failure with 5 mm min-1 speed and recorded the load and displacement were.

2.2.6. Swelling behavior of HA_tyr hydrogel

HA_tyr was dissolved at 4% (w/v) concentration in DW and mixed with hdECM at 1% (w/w). For crosslinking, SA_Ty was added in a ratio of 10:1 (HA_Tyr : SA_Ty, v/v), and hydrogel was molded with PDMS mold having a hole (d:8mm, h:2mm). After fully cross-linked, the hydrogel was dipped into PBS, and measured the weight of the hydrogel was. The swelling ratio was calculated by following the equation (Ws-Wd)/Wd, where Wi and Ws are the weights of initial and swollen hydrogel pellets.

2.2.7. Compression properties of paintable hydrogel

After swollen hydrogel pellets, Pellets were cut into similar sizes by biopsy punch with dimensions of 8 mm × 2 mm (diameter × height). The pellets were pulled to failure with 5 mm min-1 speed and recorded the load and displacement by using UTM (Shimazu, EZ-SX STD, Japan).

2.2.8. Rheological behavior of HA_Tyr hydrogel

Dynamic rheological measurements were applied to amplitude sweep and frequency sweep characteristics before and after swollen hydrogel pellets. Rheological analysis

was evaluated in the Demo lab (Anton Paar Korea) using Rheometer (MCR 302, Measuring cell: P-PTD & H-PTD 200, Measuring System: PP 25, Anton-Paar, Austria). Amplitude sweeps measured storage modulus G' and loss modulus G" as shear strain (%) increased from 0.1 to 100 at a fixed frequency of 1 Hz. Frequency sweeps measured the storage modulus G' and loss modulus G' while increasing the frequency from 0.1 to 10 Hz with 1% fixed strain.

2.2.9. Degradation behavior of HA_Tyr hydrogel

Degradation of a hydrogel is a measure of how long it retains its structure when it enters the body. The samples were molded and prepared as explained above. Degradation was evaluated by immersing in PBS and collagenase and measured for 8 hours. To see long-term degradation, degradation was observed for 4 weeks subcutaneously in CD-1 mice. Two hydrogel pellets per mouse were placed in the subcutaneous of CD-1 mice, and three mice per time condition were evaluated.

2.2.10. Live/Dead Assay

A LIVE/DEAD® Viability/Cytotoxicity Kit (Invitrogen; Waltham, Massachusetts, USA) was used to identify the viability of the cells in the medium containing the hydrogel eluate. The working solution was prepared by diluting 0.5 μM Calcein AM and 1 μM Ethidium homodimer-1 in 1 ml of PBS. After PBS washing, cells with working solution were incubated for 20 min at 37 ℃. Calcein AM was detected at the FITC (green) wavelength and EthD-1 at the TRITC (red) wavelength. All images were analyzed using a fluorescence microscope.

2.2.11. MI Modeling in Rats and Hydrogel Painting

This study was approved by the Animal Care and Use Committee of Konkuk University (IACUC NO.KU22019). All ethical codes applicable to animal experimentation and research were followed. SD rats (6 weeks old, male; ORIENTBIO INC.; Seongnam, Gyeonggi, Korea) were prepared for MI modeling. Prior to thoracotomy, rats were anesthetized with 2.5% inhaled isoflurane and an 18-gauge intravenous catheter was intubated through the trachea. At the same time, rats were mechanically ventilated with medical-grade oxygen. After adequate anesthesia for about 10 minutes, a left intercostal thoracotomy was performed. Next, the ribs were opened using a retractor, and the pericardium was removed to secure the surgical site. MI was induced by ligating the left anterior descending (LAD) artery in the heart with a 6-0 silk (Ethicon; Somerville, NJ, USA) suture. When it was confirmed that the left ventricular area (LV) had turned white following MI induction, LV was dried as much as possible using a cotton swab. Next, the prepared samples (Only Hydrogel and ECM+ hydrogel) were painted using a brush on the LV and allowed to harden for about 3 min. For Only Hydrogel, enzyme treatment was applied to previously prepared Hydrogel, and for ECM+Hydrogel, enzyme treatment was performed after mixing 1% hdECM as much as possible, and painting was performed after about 5 min of crosslinking time.

2.2.12. Masson’s Trichrome (MT) Staining

Thirty days after MI modeling, all rats were euthanized and hearts were harvested and fixed in 4% PFA. Fixed samples were embedded in paraffin after tissue processing. Then, 5 μm-sized sections were prepared using an HM 340E microtome (Thermo Fisher Scientific). Masson's Trichrome (MT) staining was performed to determine the area of fibrosis. Paraffin sections from each group were deparaffinized and fixed in Bouin's solution for overnight (O/N) at room temperature (RT). The fixed sections were stained with Weigert's iron hematoxylin solution for 10 min and with Biebrich Scarlet-acid Fuchsin solution for 15 min at room temperature. Finally, sections were stained with Aniline Blue for 5 min. Sections were continuously washed between each staining step. . CMs that survived MI are shown in red, and collagen fibers due to fibrosis are shown in blue. The percentage of fibrosis area relative to the total left ventricular wall area was quantified using ImageJ software.

2.2.13. Immunofluorescence (IF) Staining

MI-induced rat hearts were fixed with 4% PFA. Additionally, fixed hearts were soaked in sucrose for 2 days and then embedded in OCT compound. Cryosections were sliced at 9 μm thickness using the cryosectioning device at -20°C. Sections were incubated with blocking solution for 30 minutes at RT. Sections were then incubated at 4°C in primary antibody diluted in blocking solution. Primary antibodies used: anti-cardiac troponin T (cTnT; 1:200, Abcam, ab45932) and anti-α smooth muscle actin (αSMA; 1:200, Abcam, ab5694). Sections were washed three times with PBS and incubated in secondary antibody diluted in blocking solution for

2 hours at RT. Secondary antibodies used: Alexa 488 goat anti-mouse IgG (1:1000, Invitrogen, A11001) and Alexa 594 goat anti-rabbit IgG (1:1000, Invitrogen, A11012). Slides were stained with DAPI (1:100, Thermo Fisher Scientific) to identify nuclei. All images were analyzed using a fluorescence microscope, Nikon TE2000-U (Nikon; Japan) and a confocal microscope.

Chapter 3. Results and Discussions

3.1. Decellularization

3.1.1. Optimize decellularization solution concentration

In this study, SDS was used for chemical decellularization. For optimizing the chemical decellularization method which was fit in the heart tissue, the concentration of the SDS decellularization solution was determined. The lower concentration of SDS resulted in longer collagen retention, decreased ECM protein denaturation, and more cellular residues which induce rejection when dECM was implanted into the living species, while the higher concentration of SDS resulted in lower DNA content remaining in the dECM scaffolds and reduced mechanical strength. With 0.1% of SDS solution which represented the low concentration of decellularization solution, the heart remained with blood which means decellularization was performed incompletely. With 3% of SDS solution, the heart showed tissue degradation and ECM decomposition because of the high concentration of decellularization solution which is harsh condition for the heart tissue. Only, in 1% of SDS, there is less ECM decomposition than 3in % of SDS solution and decellularization was completely done. **(Figure 2, 3)**

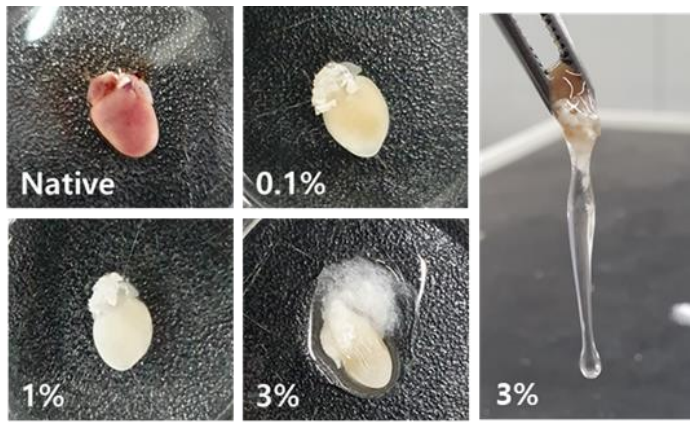

Figure 2. Optical images of native and decellularized mouse hearts

Figure 3. Optical images of native and decellularized porcine hearts

To examine heart degradation and ECM decomposition in process of decellularization, the weight remaining was measured for 48 hours of the decellularization process. Since blood was washed away during the analysis process, a slight weight loss occurred in every sample including the control sample which was dipped in the DW. The heart tissue in the 3% of SDS solution suffered from the

harsh decellularization condition and showed a dramatic decrease in the weight remaining. **(Figure 4)**

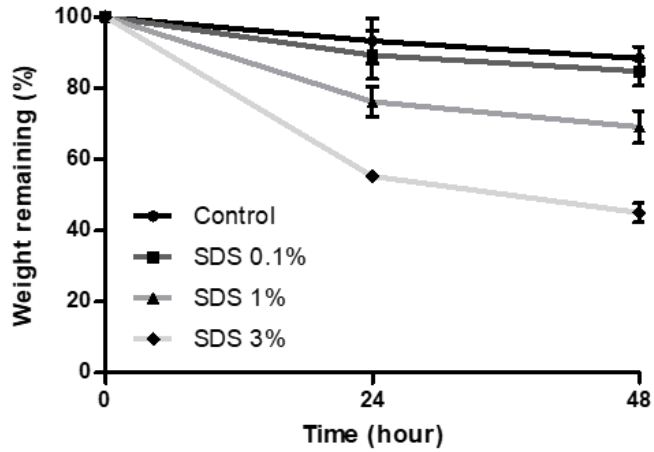

Figure 4. Weight remaining in the process of decellularization in different SDS concentrations

To confirm DNA removal and ECM remaining, H&E staining and F-actin staining were performed after paraffin sectioning. DAPI and collagen II represent nucleic acid and ECM components in F-actin staining, respectively. In the native and 0.1% SDS sample, plenty of cells that were represented by nucleic acid were remaining. (Black arrow in the H&E staining and yellow arrow in the F-actin staining) In contrast, heart tissue that was decellularized with 1% and 3% SDS solution showed complete cell removal. Nevertheless decellularized heart tissue by 3% SDS solution showed ECM decomposition which was implied through the less dense ECM. **(Figure 5, 6)**

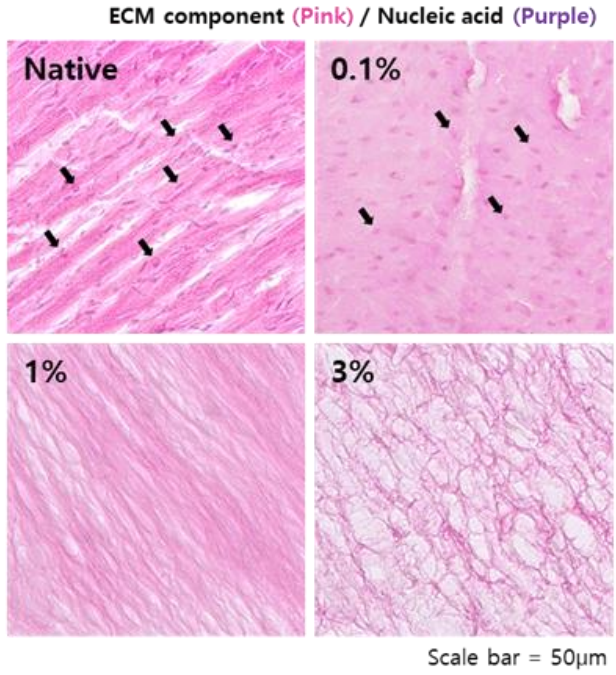

Figure 5. H&E staining of native and decellularized porcine hearts

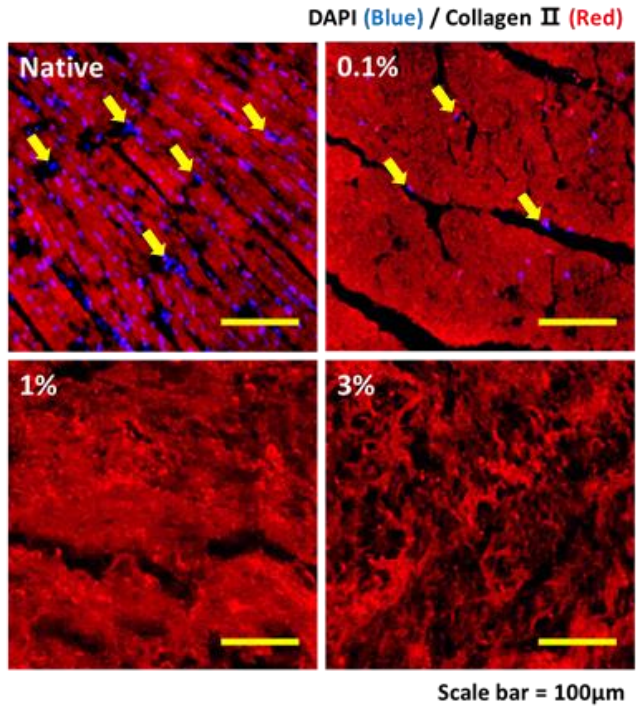

Figure 6. F-actin staining of native and decellularized porcine hearts

3.1.2. Quantification of ECM components and DNA

Through the previous results, 1% of the SDS solution was selected for the optimized decellularization solution. For detailed analysis, ECM components and DNA were quantified by several assays. GAG and collagen which are the main component of heart ECM were maintained compared with the native heart after decellularization with 1% SDS solution. Moreover, DNA quantity was dramatically decreased by over 90% and remained at only 2.56 ng/mg (Dry weight of dECM). In the previous research, dsDNA quantity lower than 50 ng/mg (ECM dry weight) indicated satisfactory cell removal from the rejection. [28] This result confirmed that 1% SDS solution met a demand for the ECM component remaining and DNA removal. **(Figure 7)** (n=3, ns>0.05, **p≤0.01, ***p≤0.001)

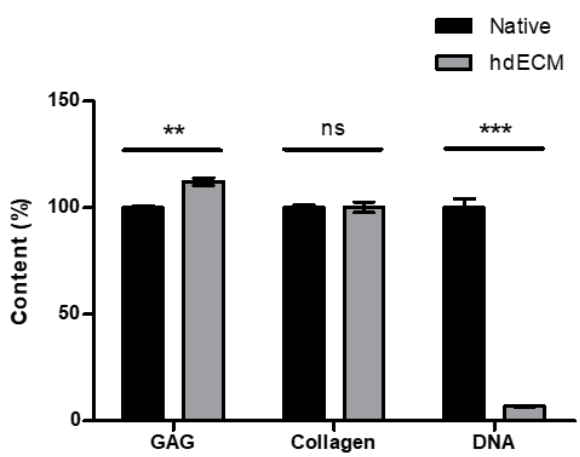

Figure 7. Quantification of ECM components (GAG and collagen) and DNA in different SDS concentrations

3.2. Paintable hydrogel

3.2.1. Synthesis of paintable hydrogel

In the previous studies, a Schiff base was formed between aldehyde-modified HA and tyramine to produce a catechol-modified HA conjugate. [29] ^{1}HNMR determined the degree of substitution (DS) after synthesis of the tyramine-conjugated hyaluronic acid (HA_tyr). The three protons in the N-acetyl group of HA appear near 2.0 ppm. Thus, the integrated area of the peak was set as three protons. Four aromatic protons in the ortho-position and meta-position of the tyramine appear between 6.8-7.2 ppm. Compared to the area of N-acetyl, the areas of protons on tyramine were 0.73 and 0.46, respectively. Based on the integrated areas of protons of the phenolic ring and N-acetyl group, the substitution rate of tyramine was calculated to be 11.8-24.0 %. **(Figure 8)** FT-IR implied conjugated tyramine moiety. The broad band at 3290 cm^{-1} corresponded to the O-H of HA. As a result of the polarization process, additional peaks appeared at 1634 and 1045 cm^{-1}, which were attributed to the C=C (aromatic) and the C-O, respectively. **(Figure 9, 10)**

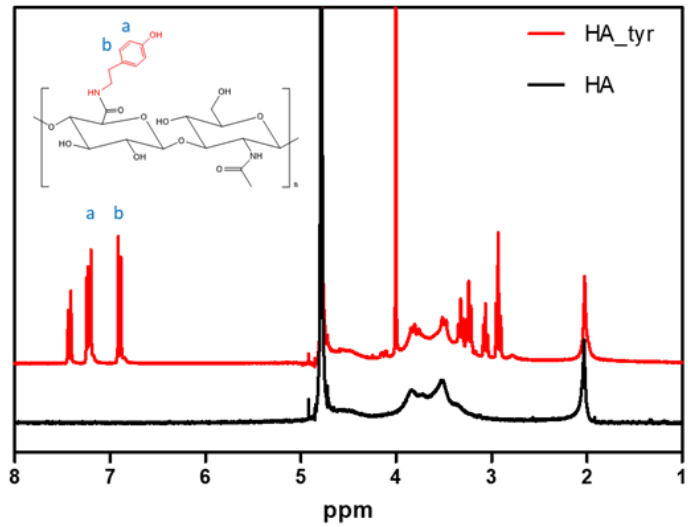

Figure 8. 300MHz HNMR of HA and HA_Tyr

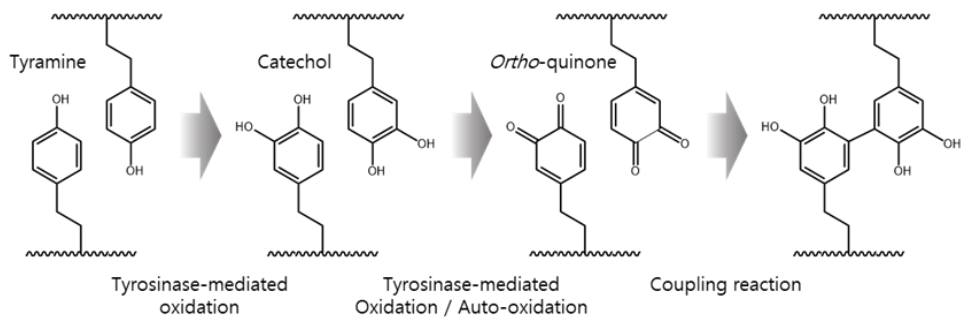

Figure 9. Mechanism of HA_tyr polarization

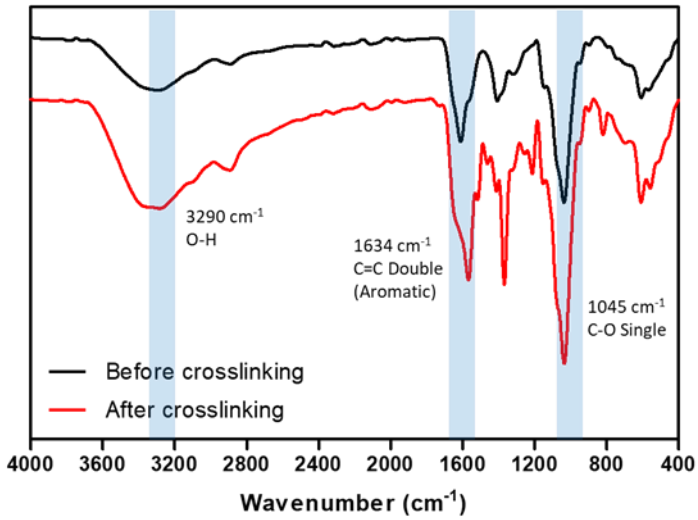

Figure 10. FT-IR of HA_Tyr and crosslinked HA_tyr

3.2.2. Specific activity of SA_Ty

Tyrosinase as an enzymatic crosslinker shows specific activity to catechol compounds. Its specific activities for monophenolic compounds (L-tyrosine and tyramine) were observed by using the Beer-Lambert law and Michaelis-Menten equation. **(Figure 11)** By measuring the reaction velocity of tyrosinase in various concentrations of monophenolic compound, values of Kcat and Km were obtained by nonlinear regression by GraphPad Prism. (n=3) **(Table 1)** Km value represents affinity to substrate and Kcat means reaction rate of formation product. Although the affinity of SA_Ty to tyramine is lower than to L-tyrosine, because of the higher reaction rate, reaction rate constants of enzyme reaction were similar in both substrates.

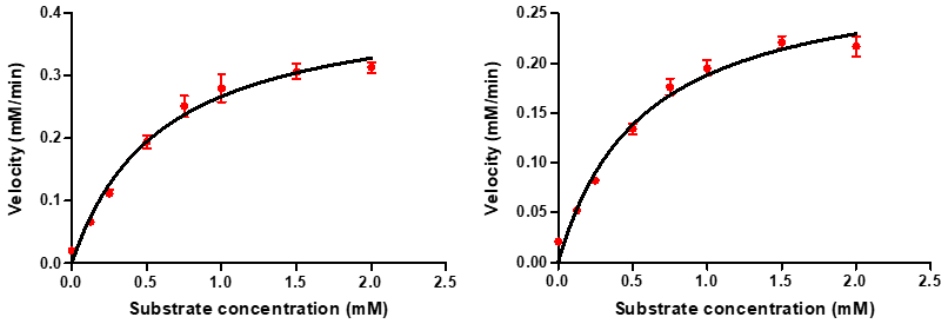

Figure 11. Specific activities of SA_Ty to monophenolic compound, L-tyrosine (Left) and tyramine (Right)

	L-Tyrosine, Monophenolase activity			Tyramine, Monophenolase activity		
	K_{cat} [S^{-1}]	K_m [μM]	K_{cat}/K_m [$M^{-1}S^{-1}$]	K_{cat} [S^{-1}]	K_m [μM]	K_{cat}/K_m [$M^{-1}S^{-1}$]
SA_Ty	0.61±0.005	524.62±23.05	0.12×10^4	1.00±0.06	780.11±23.90	0.12×10^4

Table 1. Kinetic parameters of SA_Ty for substrate L-tyrosine and tyramine.

3.2.2. Concentration optimization of paintable hydrogel

Characteristic behaviors of hydrogels, such as mechanical strength, adhesion and swelling ratio, were defined depending on the concentration of HA_tyr and the concentration of hydrogel affects to the viscosity and paintability of the hydrogel. The viscosity and paintability of HA_tyr were measured through the inverted vial test and painting, respectively. In the case of low concentrations, such as 1% and 2%, HA_tyr solutions showed rapid flow to the downside of the vial which means low viscosity. In contrast, in the case of high concentrations, such as 5% and 6%, HA_tyr solutions were ridged state with high viscosity. In the painting test with blue-colored dye, low-viscosity HA_tyr solution showed high shrinkage when they were painted

on the plastic hydrophobic sheet and high-viscosity HA_tyr solutions were painted with thick layers. Thus, in this study, 4% of HA_tyr was chosen as the optimized concentration for the paintable hydrogel. **(Figure 12)** Moreover, by using paintable hydrogel, painted on several substrates. When painted on the paper, it was painted well with a commercial brush along with making a thin hydrogel layer. And it also has adhesiveness after fully gelation. PDMS mold which has an 8mm of diameter and 2mm of height sized hole was fabricated for making commensurate pellets. By filling the PDMS mold's hole with painting hydrogel, pellets of the same size were made. Also, with painting, paintable hydrogel filled the PDMS mold's hole perfectly. **(Figure 13)**

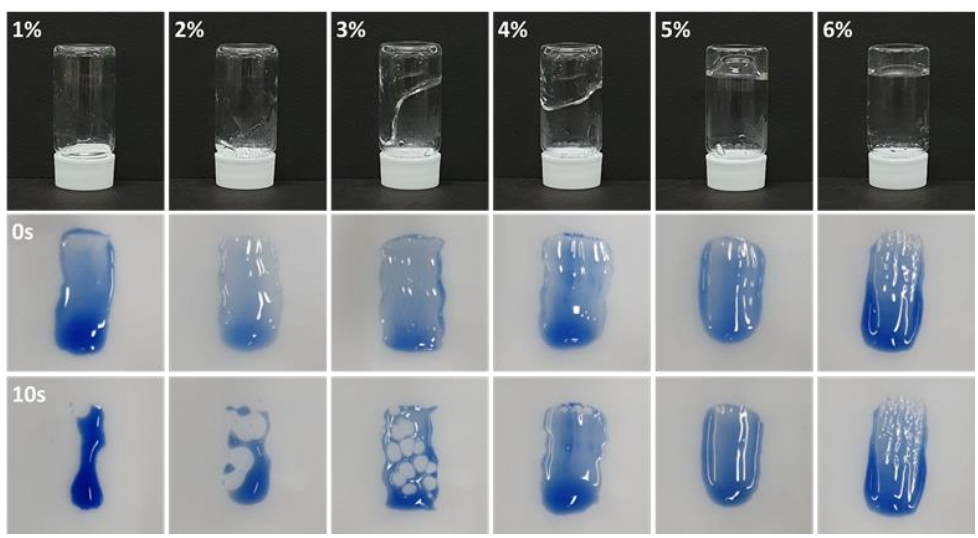

Figure 12. Paintability in the diverse concentration of HA_tyr

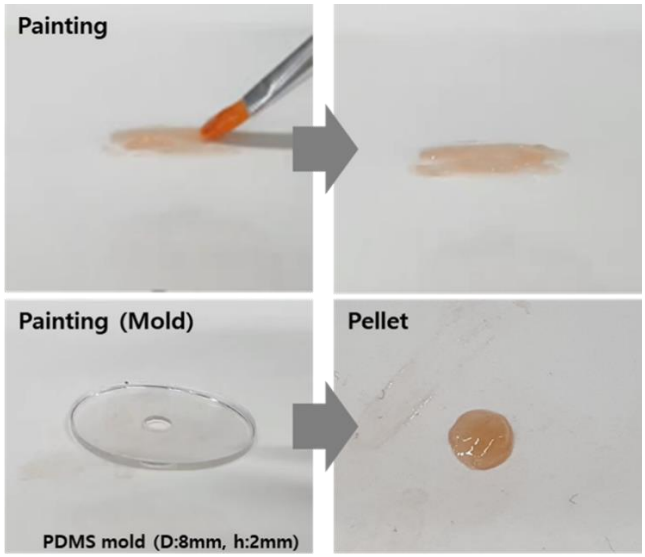

Figure 13. Painting on the paper and PDMS mold

For further analysis, an adhesion test was conducted by using UTM with several concentrations of HA_Tyr. In the case of 1% and 2% of HA_tyr-based hydrogel, they showed unmet adhesion strength. In contrast, with 4% of HA_Tyr solution, it showed the highest adhesiveness compared with the other two concentration conditions. **(Figure 14)**

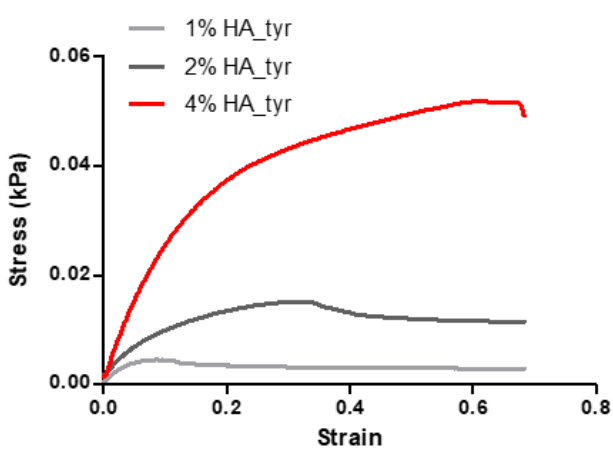

Figure 14. Adhesiveness of HA_Tyr with diverse concentration

The viscosity of hydrogel was also important to apply for paintable hydrogel. By using 4% of HA_Tyr, it still has not had enough viscosity and adhesion for paintable hydrogel. But, after adding hdECM, the hydrogel solution's viscosity was increased. It is sufficient viscosity for being painted. Finally, gelation with SA_Ty made increasing the adhesiveness of hydrogel. After fully gelation, it is hard to paint. So that, paint hydrogel when gelation was almost done near 70-80%. And then, gelation was done within 5 mins after painting. In conclusion, the hydrogel behaves as a soft and sticky paste that was flowable with sufficient viscosity at the early stage of gelation by SA_Ty and can thus be easily painted. This characteristic showed a unique advantage in that it can be painted in the form of a hydrogel for in vivo administration due to its strong adhesive force in the early stage of gelation and can be reshaped to fit complex tissue shapes. **(Figure 15)**

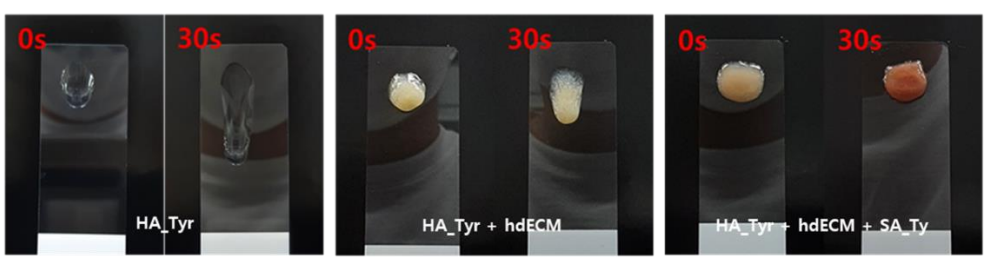

Figure 15. Viscosity of each step of HA_tyr gelation

3.2.3. Swelling property of the paintable hydrogel

For hydrogels, swelling behavior is one of the important properties. Some hydrogels need high swelling ratio for the role of drug carrier and other hydrogels with low swelling ratio suit applications that require sustained mechanical strength. In the case

of paintable hydrogel applied to the MI-induced heart, even if the swelling ratio is low, the mechanical strength should be high. For this reason, both hydrogels with and without hdECM were conducted the swelling test. In the case of hydrogel without hdECM (0% hdECM), it showed dramatic increasing swelling ratio with the increased size of the swollen hydrogel. On the contrary, hydrogel with hdECM (1% hdECM) had slight size difference after swelling and swelling ratio. **(Figure 16, 17)**

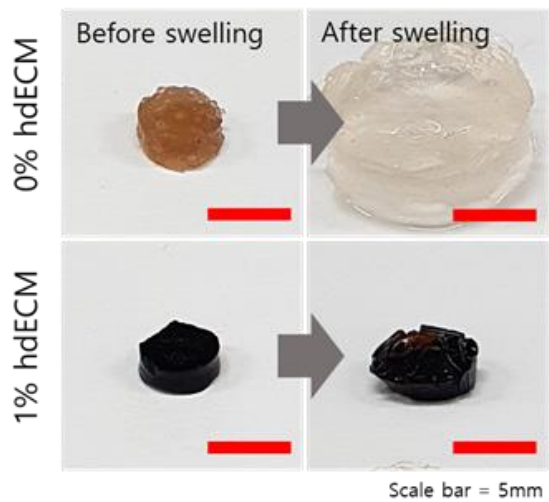

Figure 16. Swelling behaviors of paintable hydrogel pellets

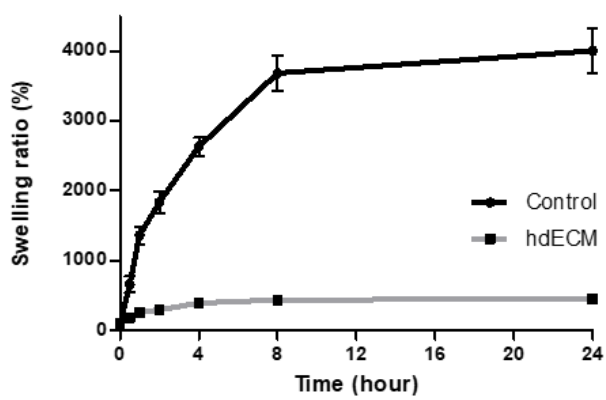

Figure 17. Swelling ratio of paintable hydrogel pellets

3.2.4. Mechanical strength of the swollen paintable hydrogel

For further analysis, mechanical properties were measured of hydrogels before and after swelling. Compressive strength measurement was conducted with similar size of paintable hydrogel pellet which had 8 mm × 2 mm (diameter × height) size. In the 0% hdECM group, loss of compressive strength after swelling was observed compared with 1% hdECM which maintained higher mechanical strength after swelling. It confirmed that the higher swelling ratio caused lower mechanical strength in the paintable hydrogel. By these results, hydrogel with hdECM still helps heart beating after being applied on MI with no mechanical changes by swelling in in vivo conditions. **(Figure 18)**

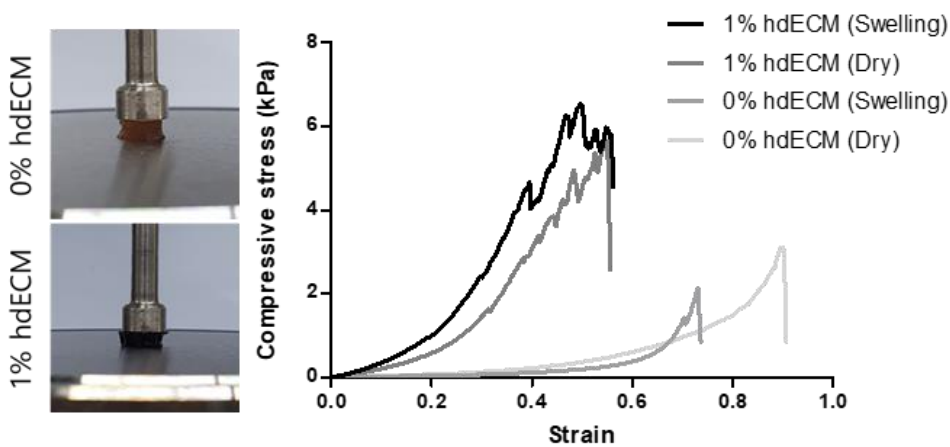

Figure 18. Compressive strength of the paintable hydrogel

For the rheological characterizations of painting hydrogel before and after swelling, amplitude sweep and frequency sweep were measured (Figure 3E). The G' of the hydrogel was higher than the G" in the entire frequency range, indicating that the

hydrogels were stable and behaved as a viscoelastic in both groups. Similar to the compression analysis, the 1% hdECM group showed higher strength before and after swelling and maintained mechanical strength. Moreover, the hdECM-containing hydrogel can give mechanical support to the ischemic heart with less mechanical strength difference by swelling in humid in vivo conditions. **(Figure 19, 20)**

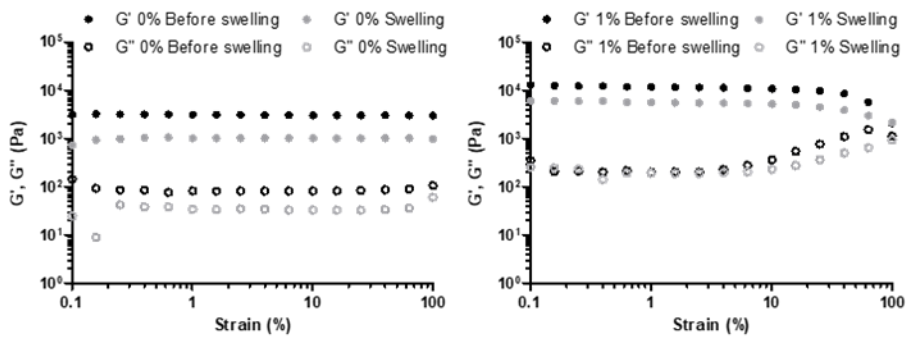

Figure 19. Amplitude sweep in rheological analysis

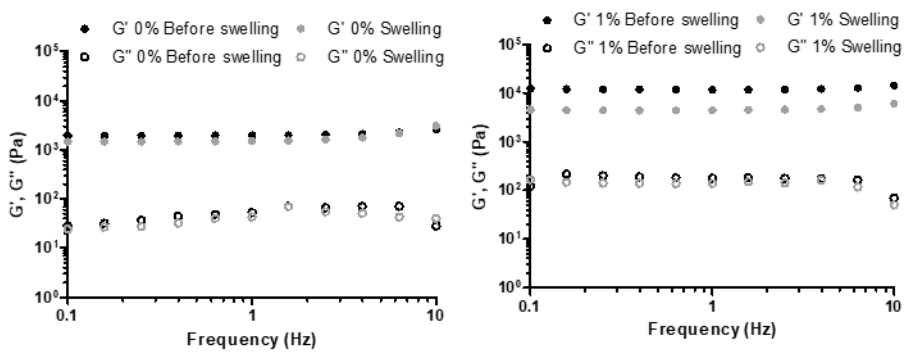

Figure 20. Frequency sweep in rheological analysis

3.2.5. Adhesion loss of paintable hydrogel

Proper adhesiveness was an essential property of hydrogels. With excessive adhesion property, hydrogel can be attached to nearby organs, such as rib cage, lung, after

being painted on MI-induced myocardium. In the case of paintable hydrogel which was crosslinked by oxidized catechol group with SA_Ty, simple wash can eliminate hydrogel adhesiveness by removing radicals that occur in crosslinking and adhesion. And this property prevents unexpected adhesion to nearby organs. Thus, after fully crosslinked and adhesion, washing step was added to remove surface adhesion of the opposite side of the left ventricular wall when the in vivo test was performed. **(Figure 21)**

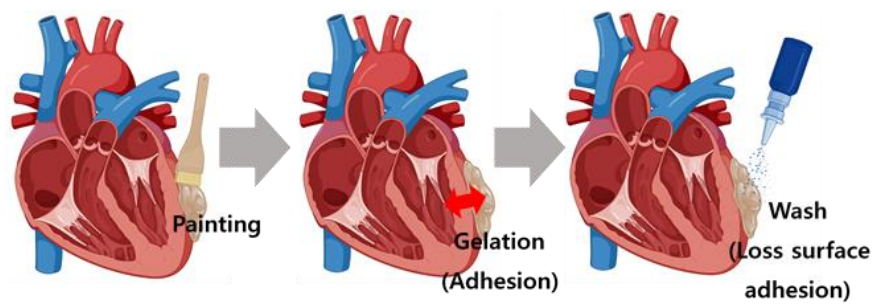

Figure 21. Scheme of losing surface adhesion of paintable hydrogel

With a simple washing step, radicals can be removed from the tissue adhesion process of the catechol groups. Then, catechol groups are blocked from transforming into the quinone and the adhesion properties of the paintable hydrogel were eliminated. The electron paramagnetic resonance (EPR) confirmed the quantity of the radicals. As the result, a simple washing step removed radicals over half compared with the control sample.

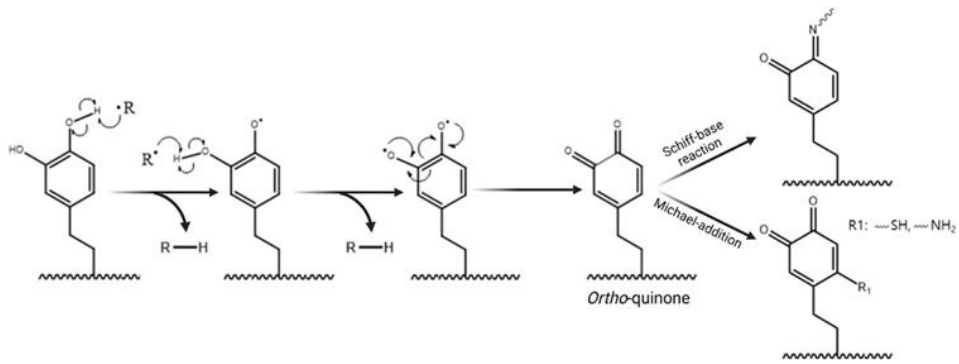

Figure 22. Tissue adhesion mechanism of the catechol group

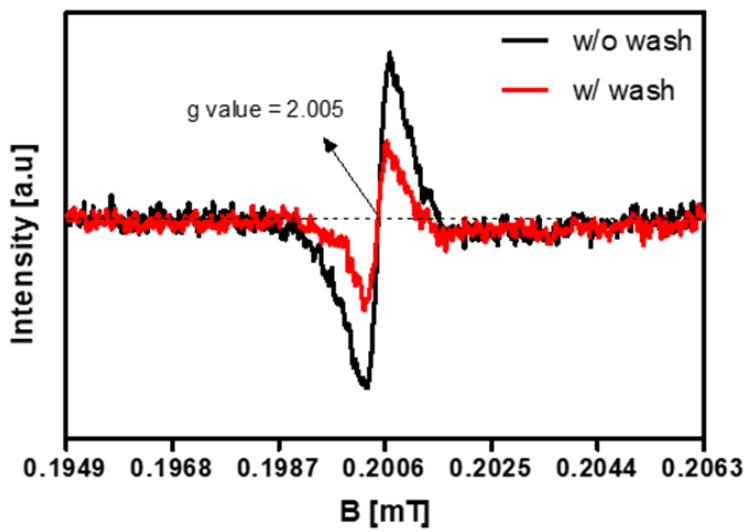

Figure 23. Quantification of radicals with or without washing

For confirmed this property, simple adhesion test was performed with paintable hydrogel with and without wash step. Before washing the paintable hydrogel pellet has adhesiveness that adheres to both sides of the finger and weighing dish. However, after washing the paintable hydrogel pellet, it lost adhesiveness on both sides. So that, it couldn't attach to any of the finger and weighing dish.

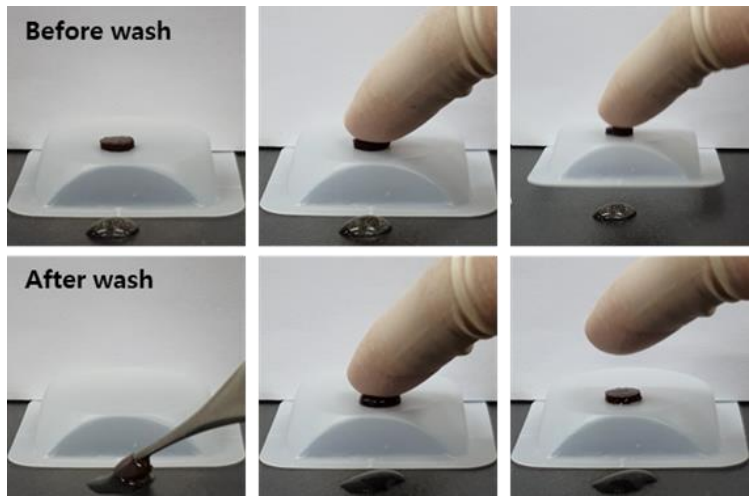

Figure 24. Adhesion test of paintable hydrogel on the weighing dish

For the details, the paintable hydrogel was analyzed adhesiveness with UTM. Though with and without hdECM hydrogel still showed high adhesiveness, paintable hydrogel with wash step completely lose its' adhesiveness. Because of that, the adhesiveness of paintable hydrogel with the wash step was nearly the same with 0kPa.

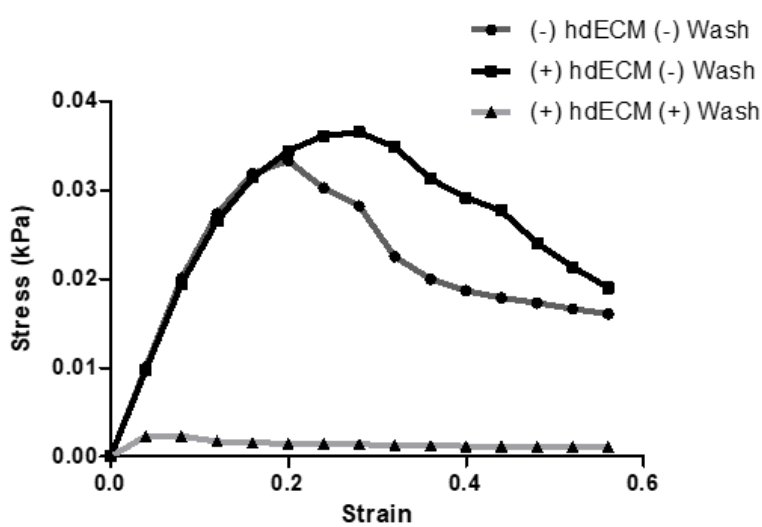

Figure 25. Adhesive strength of the paintable hydrogel

3.2.6. Radical scavenging activity of paintable hydrogel

As mentioned in figure 22, catechol groups transform into the quinone form through radical-mediated reactions. Because of this mechanism, catechol scavenges the reactive oxygen species (ROS), which increases the inflammation in the MI-induced region. Through the DPPH radical scavenging assay, every paintable hydrogel component and paintable hydrogel showed scavenging effects. **(Figure 26)**

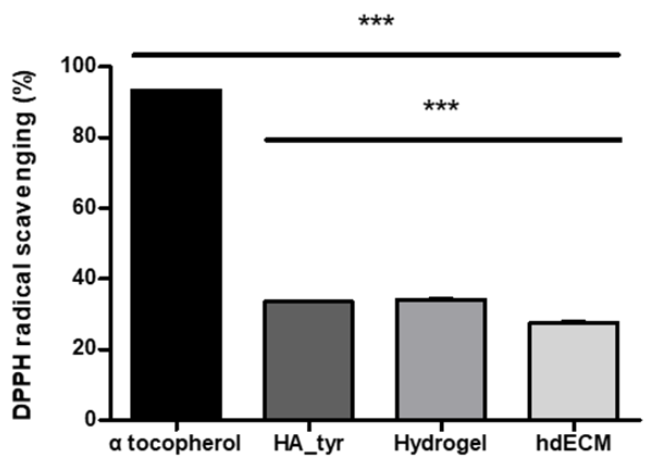

Figure 26. Radical scavenging of paintable hydrogel compounds

3.3. In vitro analysis

3.3.1. Cell viability

Implanted scaffolds should not cause the toxic response in the applied species. Thus, the cytotoxicity of hydrogel was evaluated by the Live/Dead assay with medium

extract from the hydrogel pellet. After 5 days of culture of cardiomyoblast, the hdECM-containing hydrogel group showed high cell viability which was similar lever compared with the control group indicating that hydrogel will not occur any inflammatory reaction or rejection after being applied on the MI region. **(Figure 27, 28)**

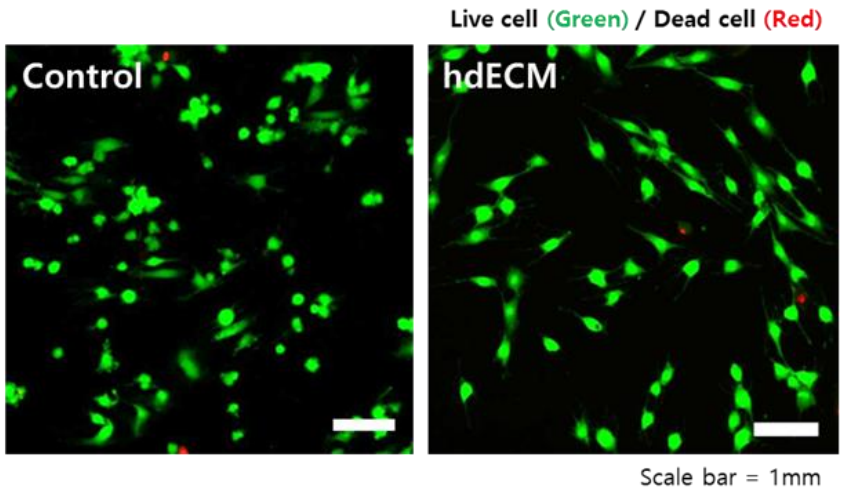

Figure 27. Live dead assay with paintable hydrogel extract

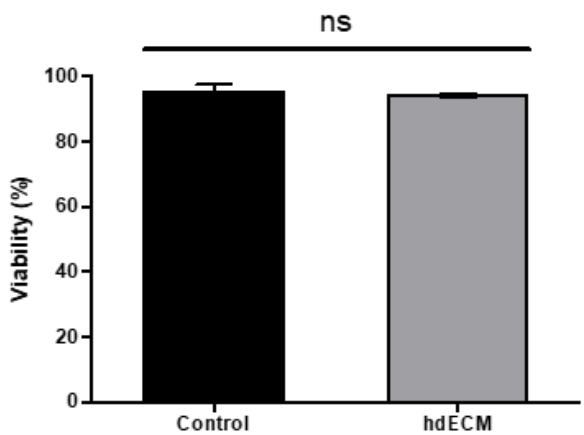

Figure 28. Cell viability ratio with paintable hydrogel extract

3.3.2. Cell differentiation

hdECM scaffold, tissue-specific dECM, could regulate cardiomyocyte proliferation and differentiation. [21] The differentiation form of cardiomyoblast was myotube, which is oriented in the same direction and has elongated shape, in certain differentiation condition. These two parameters of differentiation, cell orientation and elongated form, were observed with β-actin staining. In the hdECM group, highly oriented cell and lower circularity, which indicated elongated cells, was observed. **(Figure 29)**

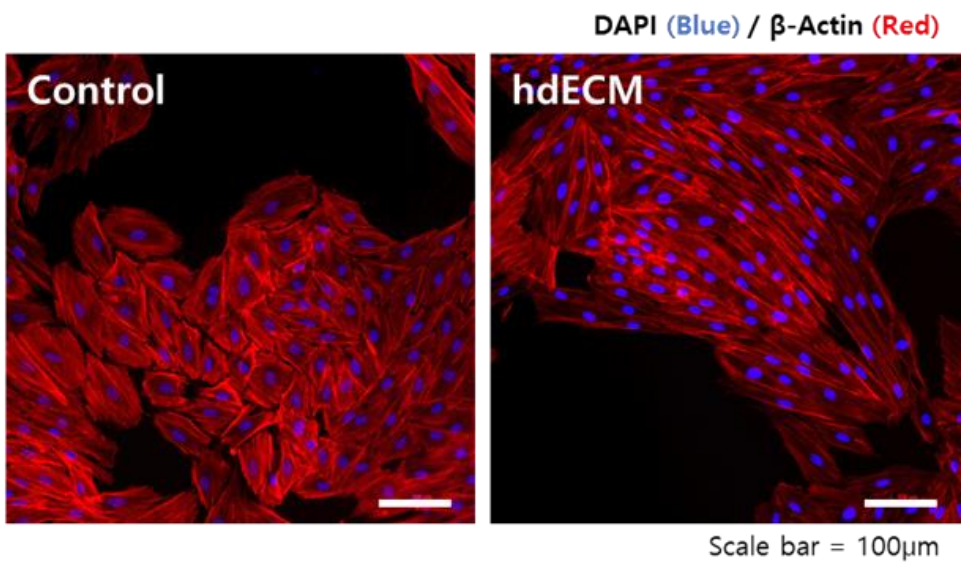

Figure 29. Differentiation of cardiomyoblast with paintable hydrogel extract

Two main standards can determine the differentiation of cardiomyoblast. First, differentiation of cardiomyoblast was determined by cell orientation. After cardiomyoblasts are differentiated, cardiomyoblasts are oriented in the same

direction to make myotube bundle. By measuring the orientation of cardiomyoblast with and without hdECM added paintable hydrogel extract, only previous cases showed similar orientation. **(Figure 30)** Second, differentiation of cardiomyoblast was determined by cell circularity. After cardiomyoblasts are differentiated, cardiomyoblasts are elongated similar to myotube. By measuring the circularity of cardiomyoblast with and without hdECM added paintable hydrogel extract, control which culturing with growth medium showed higher circularity than hdECM hydrogel extract. It means that, with growth medium, cardiomyoblast couldn't be differentiated to myotube. In contrast, cardiomyoblast with hdECM hydrogel extract could. **(Figure 31)**

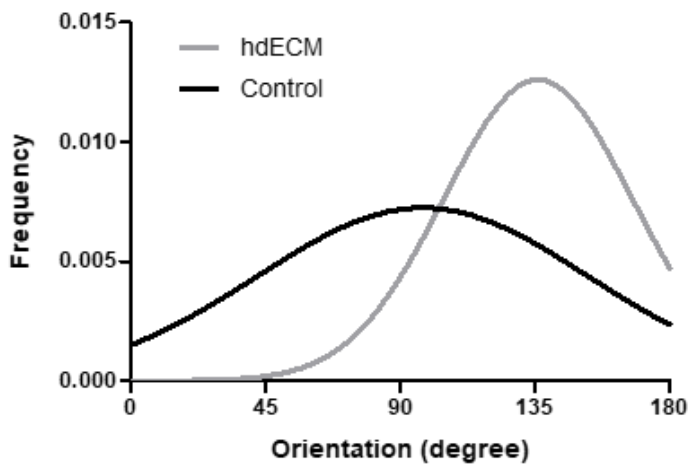

Figure 30. Cell orientations of cardiomyoblast

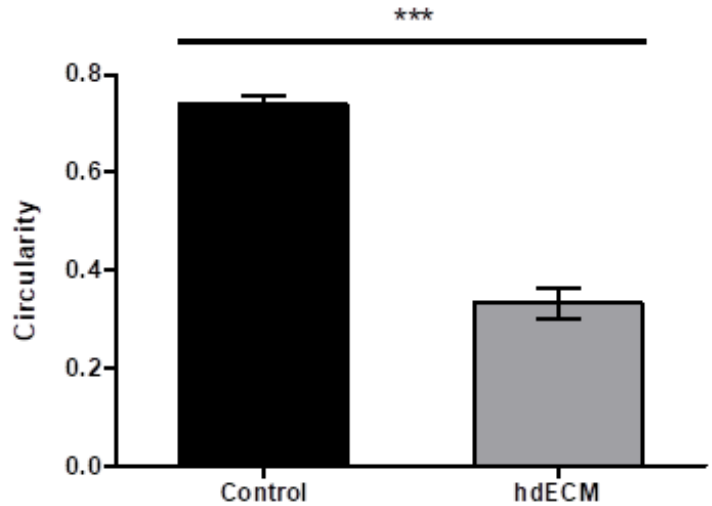

Figure 31. Cell circularity of cardiomyoblast

3.4. In vivo analysis

3.4.1. Degradation behaviors of paintable hydrogel

Before conducting in vivo analysis, defining degradation behaviors make sure that applied hydrogel gives clinical effects along with sustained shape and adhesiveness is essential. In vitro short-term degradation was conducted in the PBS and collagenase solution for 8 hours. In both cases, hydrogels were maintained at over 80% compared with initial weight. Even, in the case of hydrogel in PBS, it showed slight degradation in the 8 hours degradation test. Degradation in the collagenase was expected that degradation of hdECM contents because of the high ratio of collagen in the cardiac ECM. **(Figure 32)**

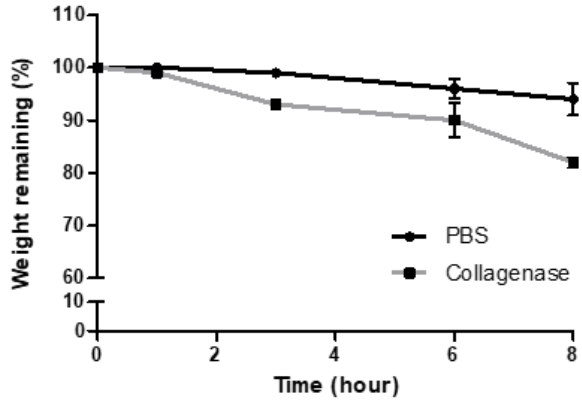

Figure 32. Weight remaining in the PBS and enzymatic condition

Degradation analysis in vivo was performed in the mice subcutaneous for 4 weeks. After 4 weeks, the measured weight remaining of hydrogel showed high maintenance, over 80%, with slightly degraded in subcutaneous. Through these results, after painting on the MI-induced myocardium, the paintable hydrogel will be maintained along with mechanical and biological support. **(Figure 33)**

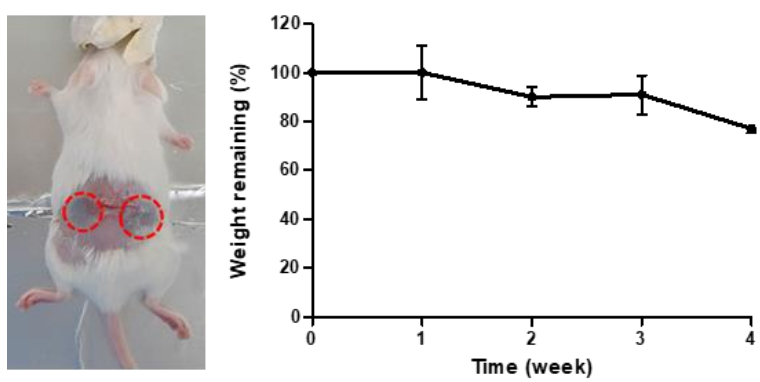

Figure 33. Weight remaining in the mice subcutaneous

3.4.2. Paintable hydrogel treatment on the MI-induced heart

With the paste state of paintable hydrogel in an early stage of gelation, it can thus be easily painted and bonded onto the rounded tissue surface in humid and beating states. After tying the left coronary artery to induce MI, the hydrogel was painted on the MI-induced myocardium, for comparison, another MI-induced rat had any treatment after MI inducing. Any secondary damage was observed to MI-induced myocardium during the painting and the gelation process. **(Figure 34)**

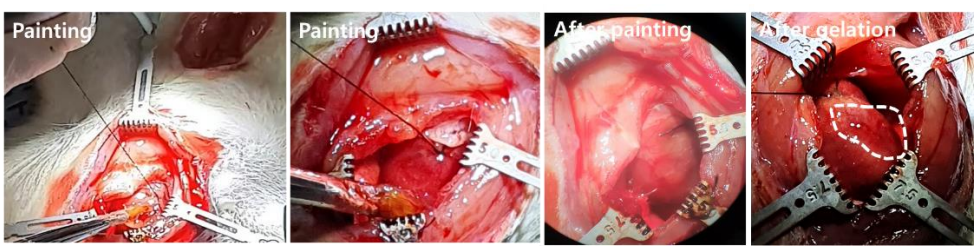

Figure 34. MI-inducing and paintable hydrogel treatment

After 4 weeks, analysis was performed. After 4 weeks from the paintable hydrogel treatment, MI induced rat was sacrificed for analysis. By observation, PBS treated MI induced heart showed necrosis of heart tissue because of blocking blood flow which is induced by MI and showed significant deterioration and severe infarction enlargement. But, in the case of paintable hydrogel treated MI induced heart, the heart showed any symptom or appearance of necrosis. And paintable hydrogel was not degraded and was well attached to the MI-induced rat heart. **(Figure 35)**

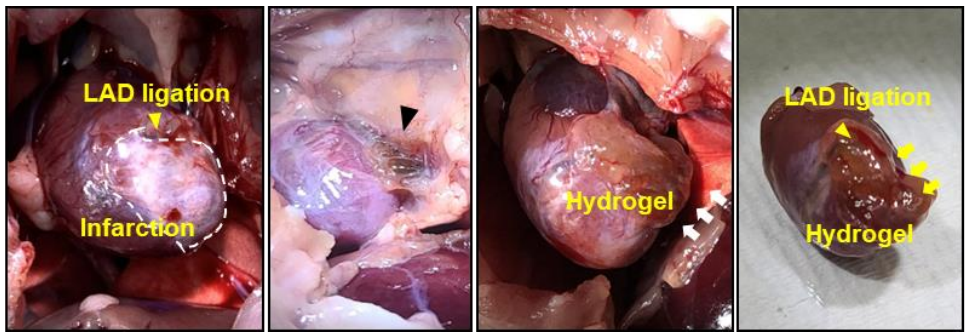

Figure 35. Induced MI and hydrogel-painted region

3.4.3. Histological analysis

After sacrifice, the infarct size and fibrosis were investigated pathologically for the PBS group, and MI group, using Masson Masson's Trichrome staining (MT staining) method Blue colored staining showed collagen and red-colored staining showed nucleic acid which means that represents cells. In the case of PBS treated MI induced heart, thinning of the LV wall was observed and significant deterioration and severe infarction enlargement. In contrast, paintable hydrogel-treated MI-induced heart showed any of thinning of the LV wall. It means that when the hydrogel is smeared within the myocardium, it reduces wall stress and the size of the left ventricular cavity, and acts as a structural support to restore the shape of the left ventricle. **(Figure 36)**

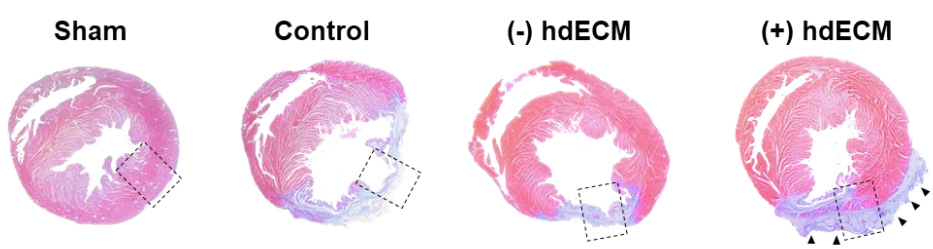

Figure 36. MT staining after 4 weeks (Whole organ)

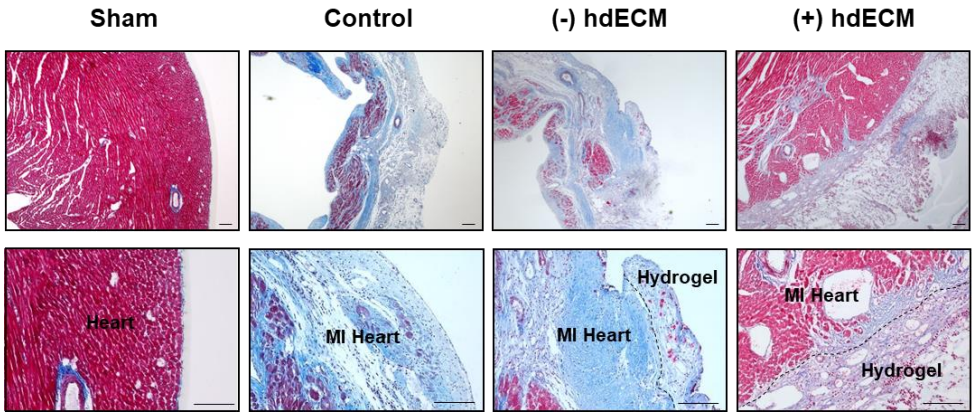

Figure 37. MT staining after 4 weeks (MI-induced region)

3.4.4. Cell infiltration and angiogenesis

The cTnT staining confirmed separation between hydrogel and MI-induced region and showed cardiomyocyte infiltration. As the result, any cardiomyocytes went into the painted hydrogel. Through αSMA staining, Vessel like structures was observed in the paintable hydrogel. It showed the possibility of angiogenesis by hdECM added paintable hydrogel. Basically, Angiogenesis helps enhance the survival of cardiomyocytes, thus reducing the risk of chronic heart failure. And Myocardial revascularization is to restore blood supply to the ischemic myocardium and to prevent the occurrence of reinfarction. [12] Moreover, the revascularization of the ischemic myocardium is critical for boosting tissue regeneration and biofunctional recovery. [5] **(Figure 38)**

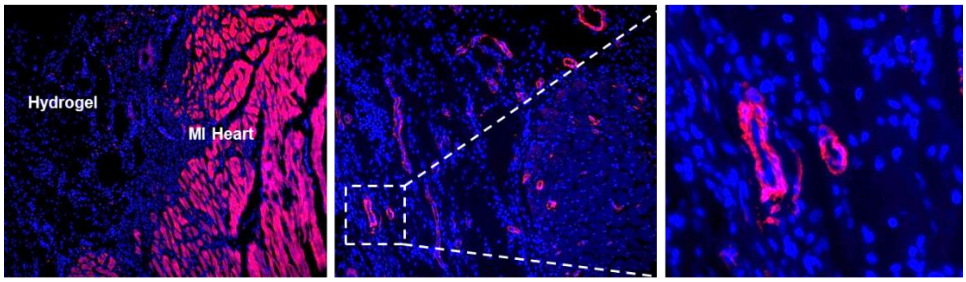

Figure 38. Cardiomyocyte infiltration and angiogenesis

3.4. In vivo analysis

After confirming paintable hydrogel on the small animal, the hydrogel was painted on the porcine heart to verify the application of scale-up. To make patterned paintable hydrogel, in ex vivo analysis, the mask was used. Without the mask, the paintable hydrogel was painted well same as applied to small animal's heart. In the same way, painting with the mask was also done well with maintaining its shape after crosslinking. These results showed that paintable hydrogel can be used for larger animal's heart. For advanced analysis of paintable hydrogel on the porcine heart. The paintable hydrogel was analyzed by two kinds of tests First, to analyze the adhesiveness of paintable hydrogel on the porcine heart, Flowed tap water to the painted hydrogel. During and after flush, the paintable hydrogel was completely maintained on the porcine heart without the occurrence of peeling off of the paintable hydrogel. Second, to mimic the heart beating condition, squeeze/stretch cycle was performed on the paintable hydrogel. In this test, paintable hydrogel also maintained its' shape and adhesiveness after the squeeze/stretch cycle. After undergoing processes such as bending, warping, soaking in water, and stretching, the hydrogel remained intact and adhered firmly to the tissue, demonstrating considerable in vivo

applicability. The remarkable bonding strength of paintable hydrogel allowed it to withstand strong water washing even with myocardial tissue and glass substrates. **(Figure 39)**

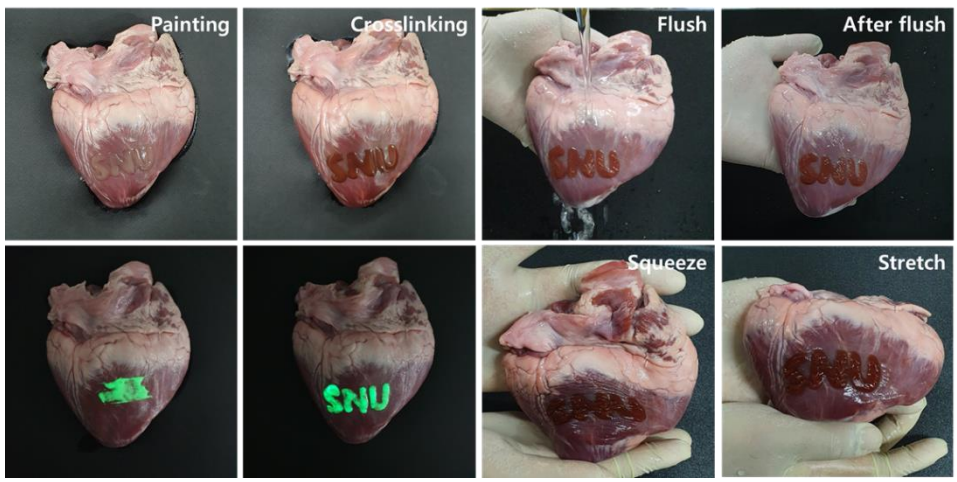

Figure 39. Paintable hydrogel adhesiveness on the porcine heart

Chapter 4. Conclusion

In this article, synthesis of the paintable hydrogel with hdECM for the MI model was the main thesis. Paintable hydrogel is selected for overcoming the limitations of injectable hydrogels and patch-type hydrogels which are fabricated by electrospinning or 3D printing. Paintable hydrogel causes any damage to the beating heart when it was applied and needs any additional treatment such as suturing or irradiation. Simply painting on the surface of the heart would certainly be more feasible approach to the clinical treatment of MI. In the synthesis of HA_Tyr which is the main component of paintable hydrogel, HA was biocompatible material and component of ECM. Tyramine has catechol group and oxidized catechol groups transformed into catechol quinone which can react with various functional groups. Also, catechol groups into the HA backbone can increase HA mechanical properties and adhesiveness Moreover, SA_Ty, enzymatic crosslinker, was used for oxidizing catechol groups. To advance paintable hydrogel for MI, tissue-specific d ECM was added to the hydrogel. Paintable hydrogels properties are confirmed by adhesion test, swelling ratio and so on. By those results, paintable hydrogel which was based on hdECM and HA_Tyr was adequate for MI treatment. Furthermore, in vitro tests confirmed that paintable hydrogel occurs less inflammation reaction and rejection and cardiac dECM regulates myocyte proliferation Through the in vivo tests, the paintable hydrogel was maintained for the long term in MI condition, prevented thinning of the LV wall and promotes revascularization of the MI region Finally, the paintable hydrogel has potential to apply on porcine or human MI which was proved by ex vivo tests.

References

1. Capulli, A., et al., *Fibrous scaffolds for building hearts and heart parts.* Advanced drug delivery reviews, 2016. **96**: p. 83-102.
2. Laflamme, M.A. and C.E. Murry, *Heart regeneration.* Nature, 2011. **473**(7347): p. 326-335.
3. Zhang, X., et al., *Decellularized extracellular matrix scaffolds: Recent trends and emerging strategies in tissue engineering.* Bioactive materials, 2022. **10**: p. 15-31.
4. Wassenaar, J.W., et al., *Evidence for mechanisms underlying the functional benefits of a myocardial matrix hydrogel for post-MI treatment.* Journal of the American College of Cardiology, 2016. **67**(9): p. 1074-1086.
5. Wu, T., et al., *Coadministration of an adhesive conductive hydrogel patch and an injectable hydrogel to treat myocardial infarction.* ACS applied materials & interfaces, 2019. **12**(2): p. 2039-2048.
6. Kang, B., et al., *Facile Bioprinting Process for Fabricating Size-Controllable Functional Microtissues Using Light-Activated Decellularized Extracellular Matrix-Based Bioinks.* Advanced Materials Technologies, 2022. **7**(1): p. 2100947.
7. Hussey, G.S., J.L. Dziki, and S.F. Badylak, *Extracellular matrix-based materials for regenerative medicine.* Nature Reviews Materials, 2018. **3**(7): p. 159-173.
8. Tsang, K.Y., et al., *The developmental roles of the extracellular matrix: beyond structure to regulation.* Cell and tissue research, 2010. **339**(1): p. 93-110.
9. Pati, F., et al., *Printing three-dimensional tissue analogues with decellularized extracellular matrix bioink.* Nature communications, 2014. **5**(1): p. 1-11.
10. Gaspar, V.M., et al., *Advanced bottom-up engineering of living architectures.* Advanced Materials, 2020. **32**(6): p. 1903975.
11. Gao, G., et al., *Tissue-engineering of vascular grafts containing endothelium and smooth-muscle using triple-coaxial cell printing.* Applied Physics Reviews, 2019. **6**(4): p. 041402.
12. Liang, S., et al., *Paintable and rapidly bondable conductive hydrogels as therapeutic cardiac patches.* Advanced Materials, 2018. **30**(23): p. 1704235.
13. Engler, A.J., et al., *Embryonic cardiomyocytes beat best on a matrix with heart-like elasticity: scar-like rigidity inhibits beating.* Journal of cell science, 2008. **121**(22): p. 3794-3802.
14. Kim, S.-H., et al., *Tissue adhesive, rapid forming, and sprayable ECM hydrogel via recombinant tyrosinase crosslinking.* Biomaterials, 2018. **178**: p. 401-412.

15. Pandey, N., et al., *Biodegradable nanoparticles enhanced adhesiveness of mussel-like hydrogels at tissue interface.* Advanced healthcare materials, 2018. **7**(7): p. 1701069.
16. Qu, J., et al., *Antibacterial adhesive injectable hydrogels with rapid self-healing, extensibility and compressibility as wound dressing for joints skin wound healing.* Biomaterials, 2018. **183**: p. 185-199.
17. Kim, J., C. Lee, and J.H. Ryu, *Adhesive catechol-conjugated hyaluronic acid for biomedical applications: A mini review.* Applied Sciences, 2020. **11**(1): p. 21.
18. Zhao, X., et al., *Physical double-network hydrogel adhesives with rapid shape adaptability, fast self-healing, antioxidant and NIR/pH stimulus-responsiveness for multidrug-resistant bacterial infection and removable wound dressing.* Advanced Functional Materials, 2020. **30**(17): p. 1910748.
19. Lee, U.J., et al., *Light-Triggered In Situ Biosynthesis of Artificial Melanin for Skin Protection.* Advanced Science, 2022. **9**(7): p. 2103503.
20. Shin, J., et al., *Tissue adhesive catechol-modified hyaluronic acid hydrogel for effective, minimally invasive cell therapy.* Advanced Functional Materials, 2015. **25**(25): p. 3814-3824.
21. Lee, F., et al., *Injectable degradation-resistant hyaluronic acid hydrogels cross-linked via the oxidative coupling of green tea catechin.* ACS Macro Letters, 2015. **4**(9): p. 957-960.
22. Lee, P.G., et al., *Circular permutation of a bacterial tyrosinase enables efficient polyphenol-specific oxidation and quantitative preparation of orobol.* Biotechnology and Bioengineering, 2019. **116**(1): p. 19-27.
23. Kim, S.-H., et al., *Hydrogel-laden paper scaffold system for origami-based tissue engineering.* Proceedings of the National Academy of Sciences, 2015. **112**(50): p. 15426-15431.
24. Yu, L. and J. Ding, *Injectable hydrogels as unique biomedical materials.* Chemical Society Reviews, 2008. **37**(8): p. 1473-1481.
25. Chang, R., J. Nam, and W. Sun, *Effects of dispensing pressure and nozzle diameter on cell survival from solid freeform fabrication-based direct cell writing.* Tissue Engineering Part A, 2008. **14**(1): p. 41-48.
26. Yuk, H., et al., *Dry double-sided tape for adhesion of wet tissues and devices.* Nature, 2019. **575**(7781): p. 169-174.
27. Jang, J., et al., *3D printed complex tissue construct using stem cell-laden decellularized extracellular matrix bioinks for cardiac repair.* Biomaterials, 2017. **112**: p. 264-274.
28. Crapo, P.M., T.W. Gilbert, and S.F. Badylak, *An overview of tissue and whole organ decellularization processes.* Biomaterials, 2011. **32**(12): p. 3233-3243.
29. Jin, Y., et al., *Injectable anti-inflammatory hyaluronic acid hydrogel for osteoarthritic cartilage repair.* Materials Science and Engineering: C, 2020. **115**: p. 111096.

Abstract in Korean

심근경색증은 심장의 관상동맥으로 가는 혈류가 감소하여 발생하는 심근 괴사로 인해 심실벽이 얇아지고 심장 기능이 상실되며 심부전이 발생하는 심혈관계 질환이다. 현재 널리 연구되는 주사 가능한 생체 재료는 주사바늘에 의한 2 차적인 조직 손상이 발생하며 치료용 패치의 경우 접착력의 부족으로 인해 봉합과정이 필요하고 이 과정 또한 2 차적인 손상을 유발한다. 이번 연구에서는 습윤한 조직 표면에서도 강한 접착성을 갖는 페인트 가능한 하이드로겔은 사용함으로써 박동하는 심장에 2 차적인 피해없이 편리하게 적용할 수 있고 안정적인 치료효과를 얻을 수 있었다. 심장 탈세포 기반 재료는 심장조직에 심장과 같은 미세환경을 제공하여 심근모세포의 분화를 유도하고 상피세포의 침투를 통해 괴사조직에 혈관을 유도하여 조직재생의 효과를 얻을 수 있었다. 타이라민 작용기가 부착된 히알루론산 기반의 페인터블 하이드로겔은 습윤한 심장 조직에도 강한 접착력을 나타내었고 적절한 팽윤율 및 심장 박동을 돕기 위한 충분한 기계적 강도를 가졌다. 또한 생체 내에서 심장 탈세포 기반 재료가 함유된 페인트 가능한 하이드로겔은 높은 안정성과 접착력으로 28 일 동안 유지되며 심근 경색 부위 심벽의 두께 감소와 섬유화를 감소시키고 혈관신생을 유도하여 효과적인 조직재생을 유도했다. 전반적으로, 페인팅이라는 간단한 방법으로 조직에 적용 가능하며 심장 조직에 특이적 환경을 갖는 심장

탈세포 기반 재료가 함유된 페인트 가능한 하이드로겔은 적절한 기계적 강도와 혈관신생 능력으로 심근 경색을 치료했다.

주요어 : 탈세포, 페인터블, 하이드로겔, 티로시나아제, 심근 경색

학번 : 2021-24083